PENNSTATE

ORNL/Sub/94-SS111/01

HIGH TEMPERATURE CORROSION OF ADVANCED CERAMIC MATERIALS FOR HOT GAS FILTERS AND HEAT EXCHANGERS

E. R. Kupp, M. F. Trubelja, K. E. Spear and R. E. Tressler

Final Report

August 1995

Report Prepared by

Department of Materials Science and Engineering
The Pennsylvania State University
101 Steidle Building
University Park, PA 16802

under

Subcontract No. 38X-SS111C

for

OAK RIDGE NATIONAL LABORATORY
Oak Ridge, Tennessee 37831

managed by

LOCKHEED MARTIN ENERGY SYSTEMS, INC.

for the

U. S. Department of Energy
under Contract No. DE-AC05-84OR21400

ORNL/Sub/94-SS111/01

HIGH TEMPERATURE CORROSION OF ADVANCED CERAMIC MATERIALS FOR HOT GAS FILTERS AND HEAT EXCHANGERS

E. R. Kupp, M. F. Trubelja, K. E. Spear and R. E. Tressler

Final Report

August 1995

Research Sponsored by the U. S. Department of Energy,
Fossil Energy
Advanced Research and Technology Development Materials Program

Report Prepared by

Department of Materials Science and Engineering
The Pennsylvania State University
101 Steidle Building
University Park, PA 16802

under

Subcontract No. 38X-SS111C

for

OAK RIDGE NATIONAL LABORATORY
Oak Ridge, Tennessee 37831

managed by

LOCKHEED MARTIN ENERGY SYSTEMS, INC.

for the

U. S. Department of Energy
under Contract No. DE-AC05-84OR21400

TABLE OF CONTENTS

TABLE OF CONTENTS (Continued)

LIST OF FIGURES

LIST OF FIGURES (Continued)

LIST OF TABLES

HIGH TEMPERATURE CORROSION OF ADVANCED CERAMIC MATERIALS FOR HOT GAS FILTERS AND HEAT EXCHANGERS*

E. R. Kupp, M. F. Trubelja, K. E. Spear and R. E. Tressler

Department of Materials Science and Engineering
The Pennsylvania State University
University Park, PA 16802

ABSTRACT

Experimental corrosion studies of hot gas filter materials and heat exchanger materials in oxidizing combustion environments have been initiated. Filter materials from 3M Co. and DuPont Lanxide Composites Inc. are being tested over a range of temperatures, times and gas flows. It has been demonstrated that morphological and phase changes due to corrosive effects occur after exposure of these materials to a simulated coal combustion environment for relatively short periods of time (10-50 hours). Heat exchanger tubes from DuPont Lanxide Composite Inc. were cut and infiltrated with Cr by heating in a Cr_2O_3 powder bed. This resulted in continuous Cr-rich layers with thicknesses ranging from 20 to 250 μm. The Cr-free and the Cr-infiltrated specimens were reacted with the molten Illinois #6 slag for 2 and 20 h at 1260°C, and the reaction layers examined with SEM and EDX. In the Cr-free specimens, the segregation of Fe and the precipitation of Fe_2O_3 were detected near the liquid/gas interface, but no evidence of corrosion was present. In the Cr-infiltrated specimens, corrosion was evident, since a rearrangement and segregation of the Cr-rich grains occurred toward the surface of the molten slag. In addition, evidence of the diffusion of major quantities of Fe was observed from the liquid slag into the Cr-rich layer formed by infiltration.

INTRODUCTION

The objectives of this work are to: (a) study the corrosion and resulting changes in mechanical properties of candidate hot gas filter materials exposed to a combustion environment, and (b) compare the corrosion effects of the Illinois #6 slag on the Cr-free and Cr-infiltrated DuPont Lanxide Composite Inc.'s SiC particulate-reinforced Al_2O_3-matrix (DLC SiC_p/Al_2O_3) composite heat exchanger materials. Our progress toward achieving these objectives is summarized below.

* Research sponsored by the U.S. Department of Energy, Fossil Energy Advanced Research and Technology Development Materials Program, DOE/FE AA 15 10 10 0, Work Breakdown Structure Element PSU-4.

SCREENING ANALYSIS OF CANDIDATE CERAMIC HOT GAS FILTER MATERIALS

Experimental Materials

The corrosion testing of ceramic hot gas filters currently involves 3M's Type 203 filters (a SiC matrix-Nextel fiber composite) and DuPont Lanxide's SiC-SiC composite filters with Nicalon fibers. In both cases the SiC matrix is produced by a chemical vapor infiltration (CVI) process. The 3M material consists of three layers. The inner layer is a two dimensional weave of Nextel 312 fibers which supports the filtering layer. The middle layer is composed of ceramic paper (a mat of chopped fibers) and the outer layer is a fishnet of Nextel 312 fibers which holds the assembly together until the CVI SiC has been deposited. Figure 1 contains scanning electron micrographs of the outer surface of the filtering layer of a 3M candle filter. In the lower magnification micrograph (Figure 1a), the random orientation of the coated fibers is evident. Figure 1b highlights the morphology of the surface of a fiber and is used for comparison with micrographs of exposed filter sections. The coatings on the fibers have a classic "cauliflower" morphology typically seen in materials produced by chemical vapor deposition (CVD). Powder x-ray diffraction of a crushed sample of the filtering layer of this material showed that it contains alpha SiC and possibly a trace of delta alumina. The SiC is probably a mixture of polytypes, but it most closely matches the powder diffraction pattern for the 15R polytype of SiC (JCPDS file number 39-1196).

The "enhanced SiC-SiC" filter from DuPont Lanxide Composites Inc. also consists of three layers. The inner layer is an open mesh of Nicalon fibers which is surrounded by a layer of Nicalon felt. A membrane on the surface comprises the outer layer and is produced by bonding SiC particulates into the interstices at the surface of the felt using a pre-ceramic polymer. Figure 2 contains micrographs of the surface of this material. The micrograph in Figure 2a was taken on the edge of a fractured surface and shows the Nicalon fibers surrounded by CVI SiC. The SiC coatings produced on these fibers are relatively smooth compared to the coatings on the fibers in the 3M composite, although they are much thicker. Again, these micrographs were used as a baseline for comparison with the morphology of the surfaces after exposure to a simulated combustion environment. As expected, phase identification of the DuPont Lanxide SiC-SiC material by x-ray diffraction shows that it contains alpha SiC. The polytype whose XRD spectra most closely matches the measured pattern is 6H (JCPDS file number 29-1128).

(a)

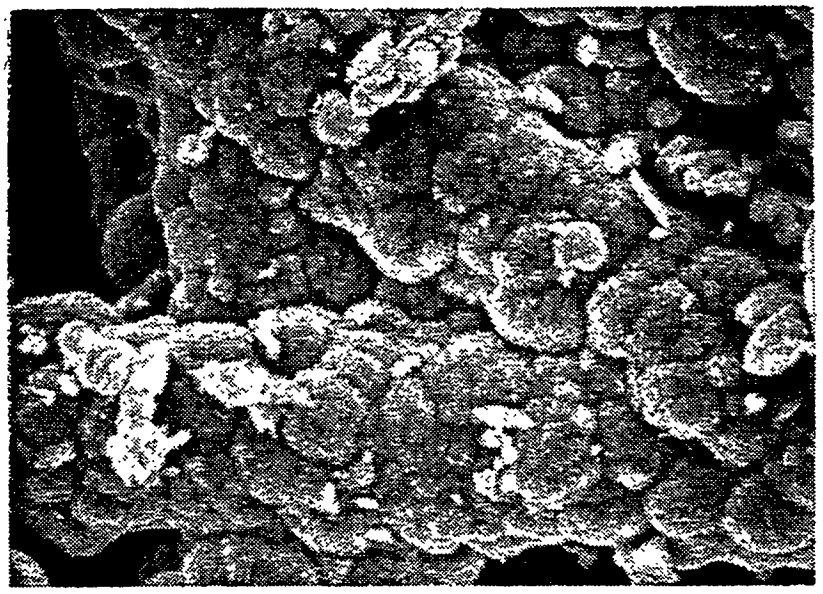

5μm

(b)

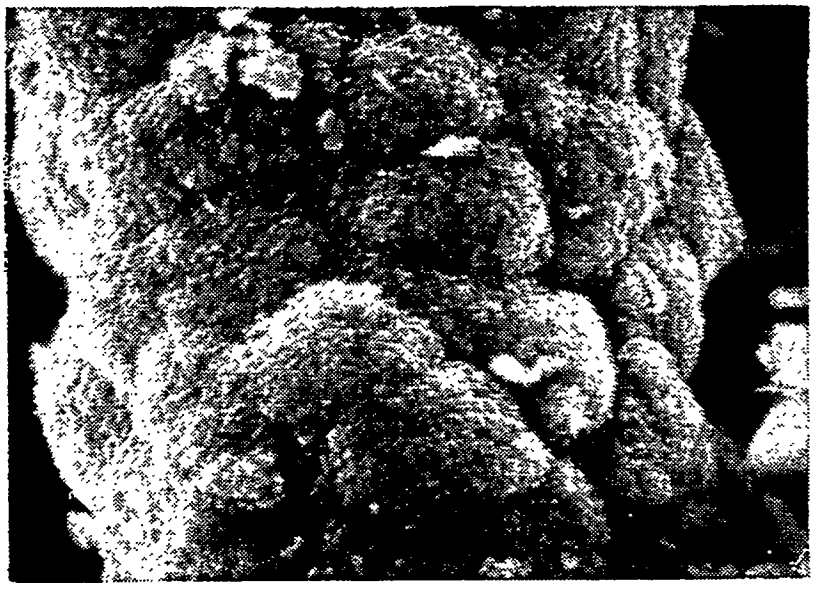

2μm

Fig.1. Scanning electron micrographs of the fibers in the filtering layer of 3M's Type 203 hot gas filter material (as-received) at two magnifications.

(a)

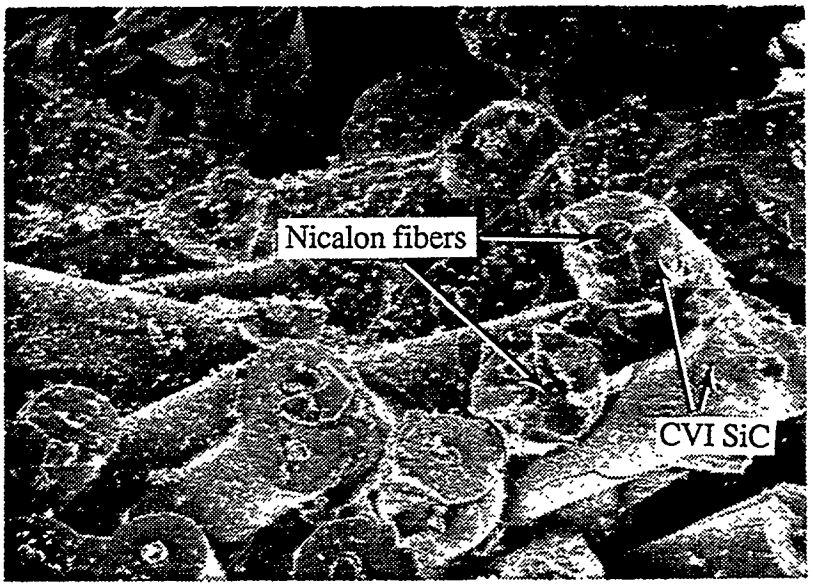

200μm

(b)

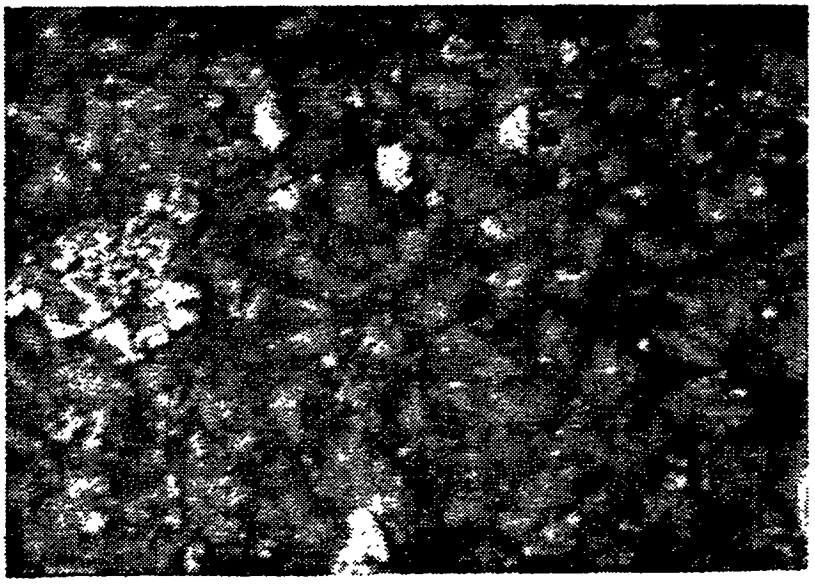

2μm

Fig. 2. Scanning electron micrographs of the fibers in the filtering layer of DuPont Lanxide's SiC-SiC hot gas filter material (as-received) at two magnifications.

The initial tests involve flow-over exposures to a combustion atmosphere of ash-coated rings cut from tubes of these materials. The ash used to coat the rings was collected at the Tidd plant and is a product of the combustion of Pittsburgh #8 coal. A parametric study of time, temperature and total gas flow was undertaken to study corrosion effects and to generate systematic corrosion data. A study of the effect of gas composition on corrosion rates was begun. The data from these tests will provide a baseline for corrosion testing of mini-candles in a flow-through configuration.

Experimental Conditions

The experimental conditions involved in the parametric study of time, temperature and gas flow are presented in Table 1. These tests are being run in a flow-over configuration as shown in the schematic diagram in Figure 3. The baseline gas composition is the same as that used at the University of North Dakota Energy and Environmental Research Center (UNDEERC), where it was determined to be representative of the combustion environment experienced by hot gas filters in a pressurized fluidized bed combustor (PFBC)[1]. These conditions were honed after discussions with various researchers involved in hot gas filter exposure work. The levels of O_2, SO_2, HCl and NaCl were chosen to maintain in one atmosphere tests the partial pressures measured at 10 atmospheres in Tidd. Since the partial pressure of water could not be maintained and levels higher than 15% are experimentally difficult to maintain, the level of water was left at its relative percentage of the gas phase. It should be noted that the level of oxygen is provided by air supplemented with oxygen.

The range of temperatures was chosen because it is representative of the conditions to which candle filters are exposed during use. Flow rates and exposure times were chosen to be practical for running laboratory tests and generating systematic corrosion data in a reasonable time frame. Short duration exposures have not been reported previously and a significant amount of corrosion may occur in the early exposure of filter materials to combustion environments.

Results and Discussion

Table 2 lists the experiments run as a fractional factorial matrix based on the conditions presented in Table 1. The experiments are listed in the order they were run (the order was randomly chosen). Corrosion effects were observed at all test conditions on

Table 1: Experimental conditions used in a flow-over configuration to study corrosion effects on filter materials in simulated coal combustion environments.

Parameter	Values
Temperature (°C)	800, 870, 950
Time (hr)	10, 25, 50
Flow rate (slm)	1, 2.5, 5
Baseline gas composition: O_2 (%)	30*
H_2O (%)	15
SO_2 (ppm)	3300
HCl (ppm)	1100
NaCl (ppm)	10
Air	Balance*

* The total oxygen level is 30%, including O_2 contributed by the air.

Table 2: Matrix of parametric tests run to study the effects of time, temperature and flow rate on corrosion of hot gas filter materials in a simulated combustion atmosphere.

Run	Time (hr)	Temperature (°C)	Flow Rate (slm)
PT1	25	800	2.5
PT2	10	870	5.0
PT3	25	870	1.0
PT4	10	950	2.5
PT5	50	800	5.0
PT6	25	950	5.0
PT7	10	800	1.0
PT8	50	870	2.5
PT9	50	950	1 .0

both materials. Observations include the color change of the ash due to exposure and the relative stickiness of the ash in addition to XRD and SEM analyses. In each case, x-ray

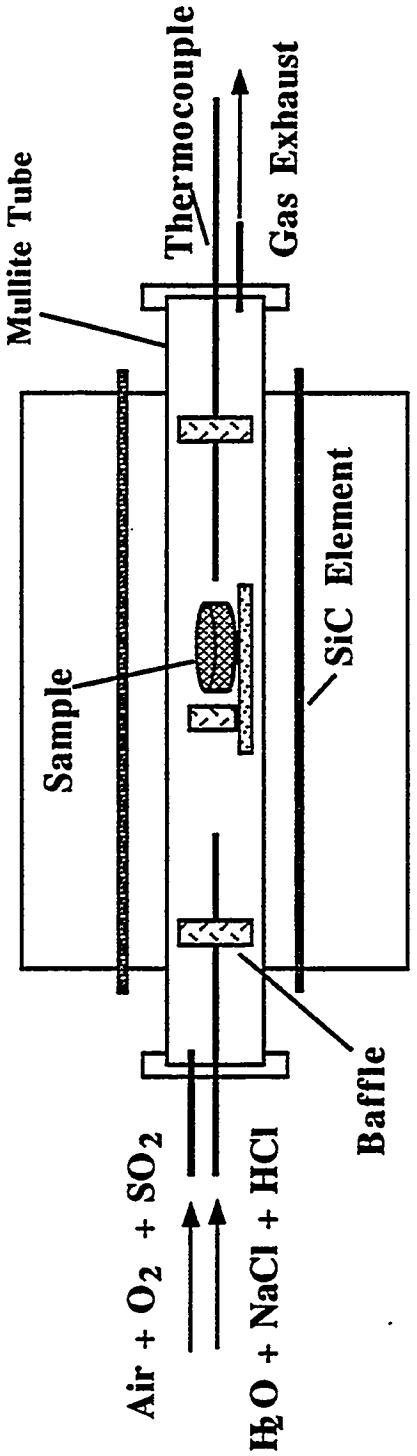

Figure 3. Schematic diagram of the flow-over furnace used for screening tests of candidate hot gas filter materials.

diffraction results showed at least the presence of an amorphous component in the filtering layer of the material. The relative height of the amorphous hump could generally be correlated with amount of glassy material observed on the fiber coatings using the SEM. When the ash was considered sticky (i.e. hard to remove from the fiber surface and formed clumps during crushing in a mortar and pestle), some minor peaks due to ash were identified on the x-ray patterns of both filter materials. The samples on which the ash was sticky also seemed to have the largest amorphous component and XRD spectra of the exposed ash showed the largest differences from the as-received ash patterns. The XRD patterns for the ash have not been completely characterized because the ash is a complex mixture of phases, but sets of peaks disappear and others appear after exposure of ash to the combustion environment. These changes are expected to correspond to the reaction of some of the original phases with the environment to form new phases. A trace amount of tridymite was also detected in samples of the DuPont Lanxide material which contained the larger amounts of amorphous material.

The morphology of the fiber coatings was also altered by the exposures. 3M's filter material exhibited separation of the grain clusters making up the film (compare the exposed materials in Figure 4 to the as-received material shown in Figure 1). It appears that material is being etched in the boundaries between the grain clusters. Other changes to this material included the precipitation and growth of submicron crystals with regular shapes (cubes and/or platelets) on the fibers after exposure to certain conditions. Examples of these crystals are shown in Figure 5. In almost all cases the presence of a glassy film was observed on the fiber surfaces, which is most likely the amorphous phase identified by XRD.

The DuPont Lanxide SiC-SiC filter material also exhibited morphological changes after exposure to a simulated combustion environment. As with the 3M material, there was a glassy layer on the surfaces of all of the samples. The surfaces of the fibers in these samples generally became smoother after exposure, whereas the 3M fiber surfaces were generally rougher after exposure. There was possibly growth of crystals on the fiber surfaces similar to those observed on the 3M filter, although the occurrence of the crystals was more sporadic and their shapes less regular (Figure 6a). In one case, submicron pin holes formed in the glassy layer which formed on the surface (Figure 6b). There are also ash particles stuck on the fibers which either sunk into this layer or around which this layer grew during exposure. Again paralleling the 3M material, the glassier the appearance of the fibers surfaces, the larger the amorphous hump in the XRD pattern for the same sample.

(a)

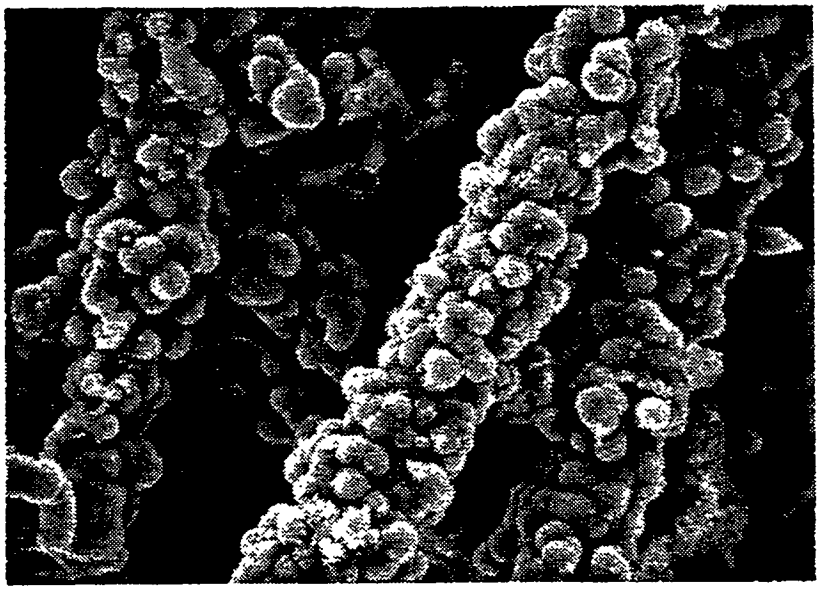

5μm

(b)

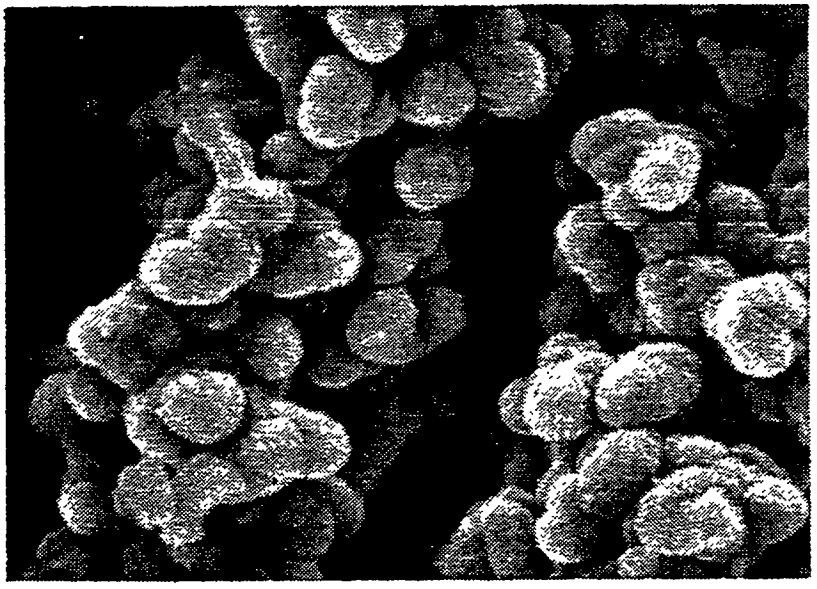

2μm

Fig. 4. Scanning electron micrographs of the fibers in the filtering layer of 3M's Type 203 hot gas filter material after exposure to simulated combustion environments in tests (a) PT4 (10 hr, 950°C, 2.5 slm) and (b) PT5 (50 hr, 800°C, 5.0 slm).

(a)

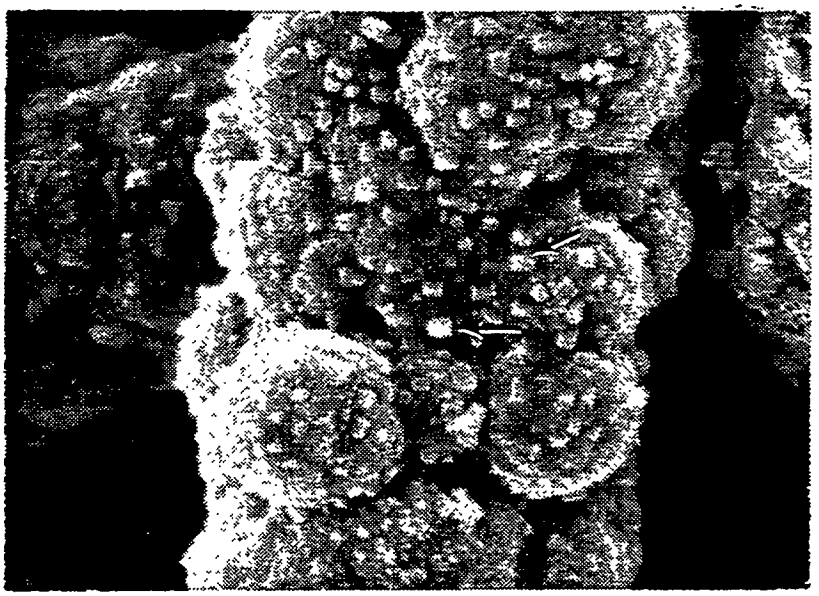

2μm

(b)

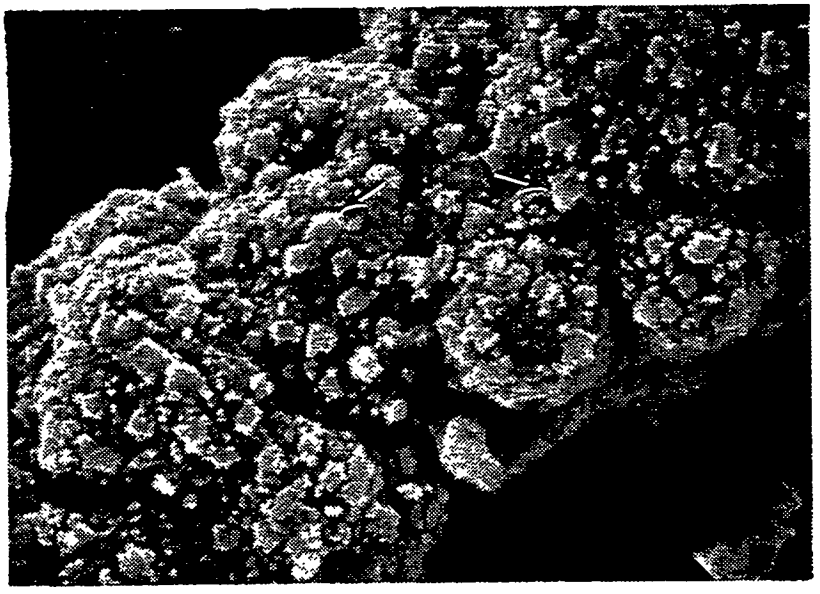

Fig. 5. Scanning electron micrographs of the fibers in the filtering layer of 3M's Type 203 hot gas filter material after exposure to simulated combustion environments in tests (a) PT2 (10 hr, 870°C, 5.0 slm) and (b) PT3 (25 hr, 870°C, 1.0 slm).

(a)

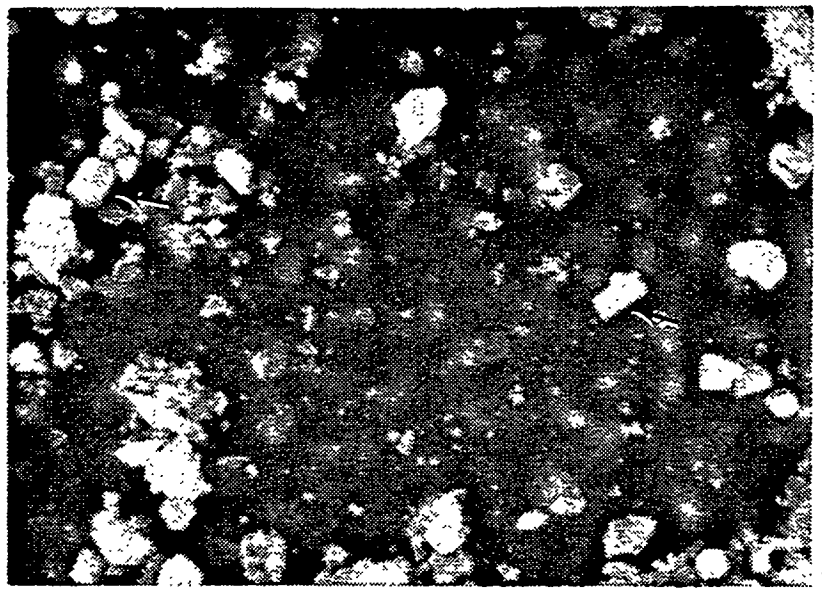

2μm

(b)

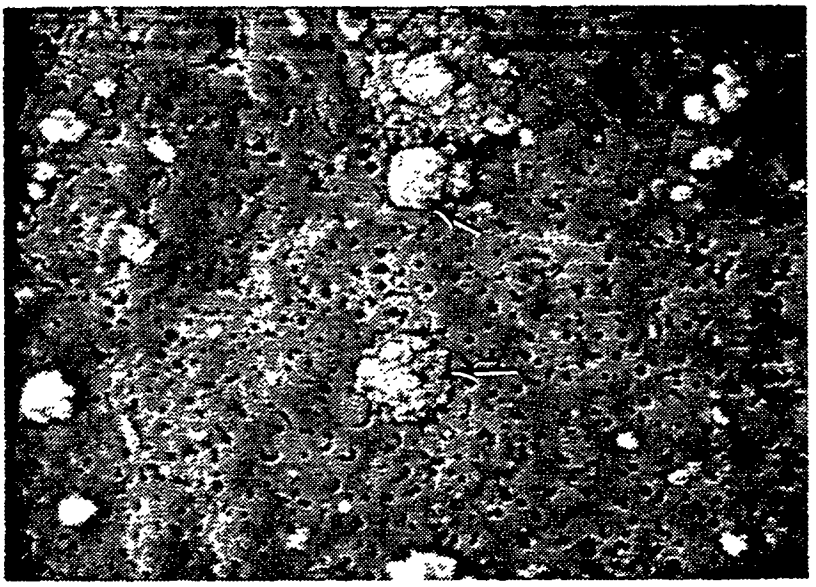

Fig. 6. Scanning electron micrographs of the fibers in the filtering layer of DuPont Lanxide's SiC-SiC hot gas filter material after exposure to simulated combustion environments in tests (a) PT4 (10 hr, 950°C, 2.5 slm) and (b) PT5 (50 hr, 800°C, 5.0 slm).

Construction of a thermochemical database containing the components of the filter materials, ash and combustion gas has been started. Thermochemical calculations will be used in conjunction with the final results of the parametric screening tests to develop an understanding of the initial stages of corrosion of the candidate materials in combustion environments. The current database contains the appropriate phases from the MICROTHERM database[2]. The calculations will be done using ChemSage[3].

Summary and Future Research on Hot Gas Filter Materials

Initial exposure testing of fiber composite hot gas filter materials from 3M Co. and DuPont Lanxide Composites Inc. has confirmed that corrosive effects are observable after short term exposure times to PFBC conditions. Morphological changes were seen on the surfaces of the coated fibers which comprise the filtering media. XRD analysis showed the presence of an amorphous component in all cases and sometimes a trace of tridymite was also observed on the DuPont Lanxide material. The presence of amorphous material correlates with the glassy or glazed appearance of the fiber surfaces observed using scanning electron microscopy. After completing analysis of the samples exposed to the conditions presented in Table 1, the results will be used in conjunction with thermochemical calculation results to develop systematic corrosion data at these combustion conditions. This experimental matrix was run on the 3M and DuPont Lanxide materials simultaneously. A second set of flow-over tests will be carried out to study the effects of varying the levels of the corrodant species in the gas phase.

Longer term (200 hour) flow-through exposures of mini candles will be initiated when the baseline corrosion data has been determined using rings of candles exposed in the flow-over tests. The experimental parameters for these tests will be chosen based on results from the flow-over tests in conjunction with thermochemical calculation results. The exposed candles will be analyzed in the same way as the rings in the flow-over tests as well as being cut into rings for mechanical property testing. The expected result will be correlations of exposure conditions with corrosion effects and mechanical properties.

CERAMIC HEAT EXCHANGER MATERIALS WITH CHROMIUM SURFACE TREATMENTS FOR CORROSION RESISTANCE

Background Information

Ceramic heat exchangers in coal-fired power plants are exposed to extremely harsh environments, with the temperatures reaching up to 1600°C and a variety of coal combustion products causing both the corrosive and erosive damage to the material.[4] A DLC SiC_p/Al_2O_3 composite has been receiving increased attention as a candidate heat exchanger material because of its favorable combination of thermal conductivity, mechanical properties (creep resistance and hot strength), oxidation/corrosion resistance in fossil fuel environments, and thermal shock resistance.[5] However, in contact with the alkali and alkaline-earth rich slags, the accelerated corrosion of the composite is likely to occur because of the formation of the low-melting silicate phases on the surface.

Chromium oxide has a very low solubility in silica and molten silicates. In addition, the corrosion rate of alumina–chromia mixtures in the $CaO–MgO–Al_2O_3–SiO_2$ melts has been found to decrease with an increase in Cr_2O_3 concentration.[6] It is, therefore, expected that the composite surface modified with Cr_2O_3 will resist liquid formation and provide improved corrosion resistance as compared to the Cr_2O_3-free composite.

The purposes of the following sections are (i) to describe two methods of infiltrating Cr into the DLC SiC_p/Al_2O_3 composite, and to present the results of the SEM and EDX analyses of the infiltrated material, indicating the extent of the Cr penetration; (ii) to compare the microstructures of the near-surface layers of the Cr-free and Cr-infiltrated DLC SiC_p/Al_2O_3 composites after exposure to the molten Illinois #6 slag for 2 and 20 h at 1260°C; and (iii) to propose another coating material for SiC heat exchanger tubes, suitable for testing the Cr-modification concept.

Experimental Procedure

Starting Material and Specimen Cutting

A series of 12.7-mm high, 60° arc-span specimens were cut with a high-speed diamond saw from the manufacturer-supplied DLC SiC_p/Al_2O_3 heat exchanger tubes (OD = 50.8 mm, ID = 41.3 mm, L = 152 mm). The tubes were fabricated from a SiC particulate preform through which an Al_2O_3/Al composite was grown by the directed

oxidation of a molten aluminum alloy (the Dimox™ process). Further details on the fabrication, microstructure and properties of the DLC SiC_p/Al_2O_3 composite have been presented elsewhere.[5, 7] The dimensions and mass of each individual specimen were measured before any further heat treatments were undertaken.

Chromium Infiltration

The chromium infiltration of the specimens was accomplished by one of two methods: (1) heating the composite in a Cr_2O_3 powder bed; and (2) heating the composite in molten $Cr(NO_3)_3 \cdot 9\ H_2O$. Prior to corrosion testing, both types of Cr-infiltrated specimens were subjected to a high-temperature heat treatment in air at 1500°C, using a bottom-loaded $MoSi_2$-heated furnace. The 1500°C heat treatment was performed to ensure Cr interdiffusion into the Al_2O_3 grains, as well as to reoxidize and homogenize the specimen surfaces. The temperature of 1500°C was selected to be somewhat higher than the maximum anticipated corrosion test temperature (1400°C),[8] thus ensuring the microstructural and compositional stability of the Cr-infiltrated specimens during the tests.

A complete description of the experimental conditions employed in methods (1) and (2) is presented in Tables 3 and 4, respectively. In method (1), the purpose of the low-

Table 3. Experimental conditions for DLC SiC_p/Al_2O_3 composite surface modification in Cr_2O_3 powder bed.

Sample No.	Infiltration Temperature/Time	Equilibration Temperature/Time
1	1000°C/2 h	1500°C/2 h
2	1100°C/2 h	1500°C/2 h
3	1100°C/12 h	1500°C/2 h
4	1100°C/12 h	1500°C/6 h

temperature heat treatment at 1000° or 1100°C was to recreate the conditions for the Dimox™ process, thereby producing simultaneous melting, growth and oxidation of residual Al within the composite. As shown schematically in Fig. 7, the Cr_2O_3 particles in the powder bed were trapped within the molten Al on the composite surfaces. In method

Table 4. Experimental conditions for DLC SiC_p/Al_2O_3 composite surface modification in molten $Cr(NO_3)_3 \cdot 9\ H_2O$.

Sample No.	Surface Modification	Cr-Nitrate Infiltration	Cr-Nitrate Decomposition	Surface Equilibration
5	1100°C/12 h	80°C/24 h + Drying*	600°C/1 h	1500°C/2 h
6	1100°C/12 h	80°C/24 h + Drying*	600°C/1 h	1500°C/6 h
7	Concentrated HCl/12 h	80°C/24 h + Drying*	600°C/1 h	1500°C/2 h
8	Concentrated HCl/12 h	80°C/24 h + Drying*	600°C/1 h	1500°C/6 h

*Room Temperature/48 h.

(2), the heat treatment at 1100°C (equivalent to the Dimox™ process) or, alternatively, the chemical treatment in concentrated HCl (by etching the residual Al) allowed for the formation of additional porosity on the specimen surfaces. The molten chromium (III) nitrate was subsequently expected to penetrate the surface pores by capillary action (Fig. 8). Prior to surface equilibration at 1500°C, the Cr-nitrate was decomposed into an oxide at 600°C.

The Cr-infiltrated specimens heat treated at 1500°C were sectioned with a high-speed diamond saw and polished with the 120, 40 and 10-μm diamond grinding wheels, followed by the 3 and 1-μm diamond polishing paste. SEM and EDX analyses of the polished cross sections were performed to verify the extent of Cr penetration and to select the specimens for corrosion testing.

Corrosion Testing

The as-cut and selected Cr-infiltrated specimens were reacted in air for 2 and 20 h at 1093° and 1260°C with the Illinois #6 slag from the Baldwin Plant. It was observed that, following the test at 1093°C, the slag was partially sintered, whereas during the heat treatment at 1260°C the slag was molten. The slag composition is summarized in Table 5.[8]

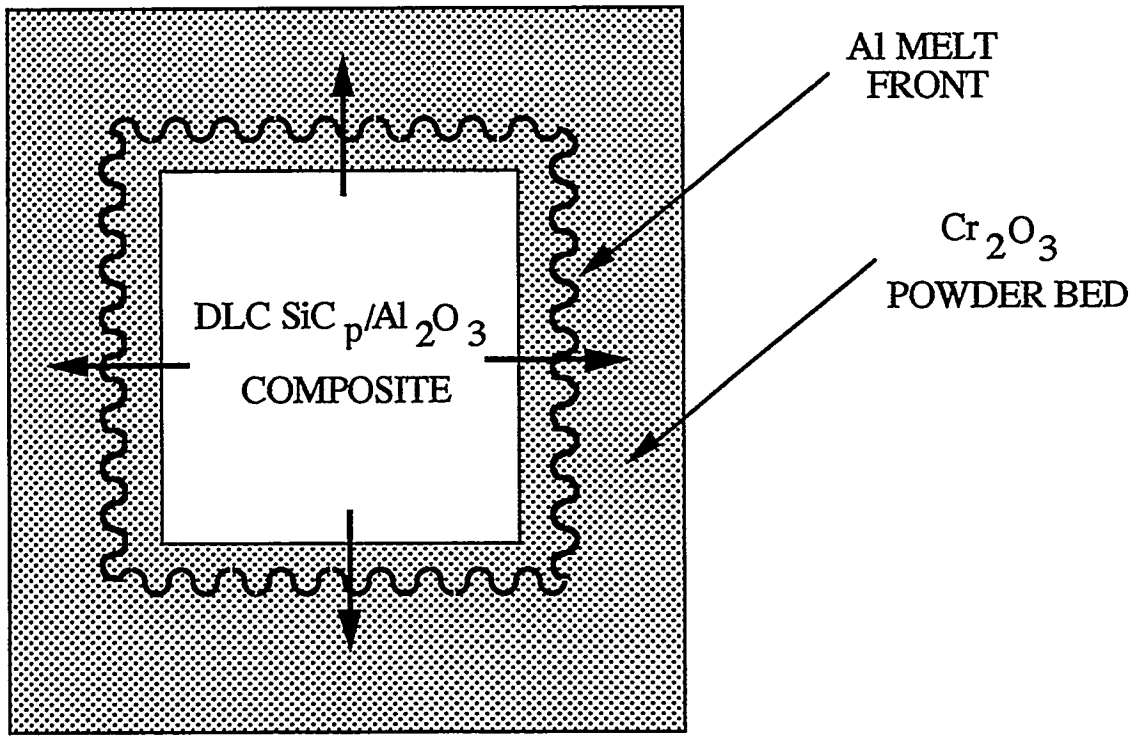

Fig. 7. Schematic of the Cr-infiltration of a DLC SiC_p/Al_2O_3 composite in a Cr_2O_3 powder bed.

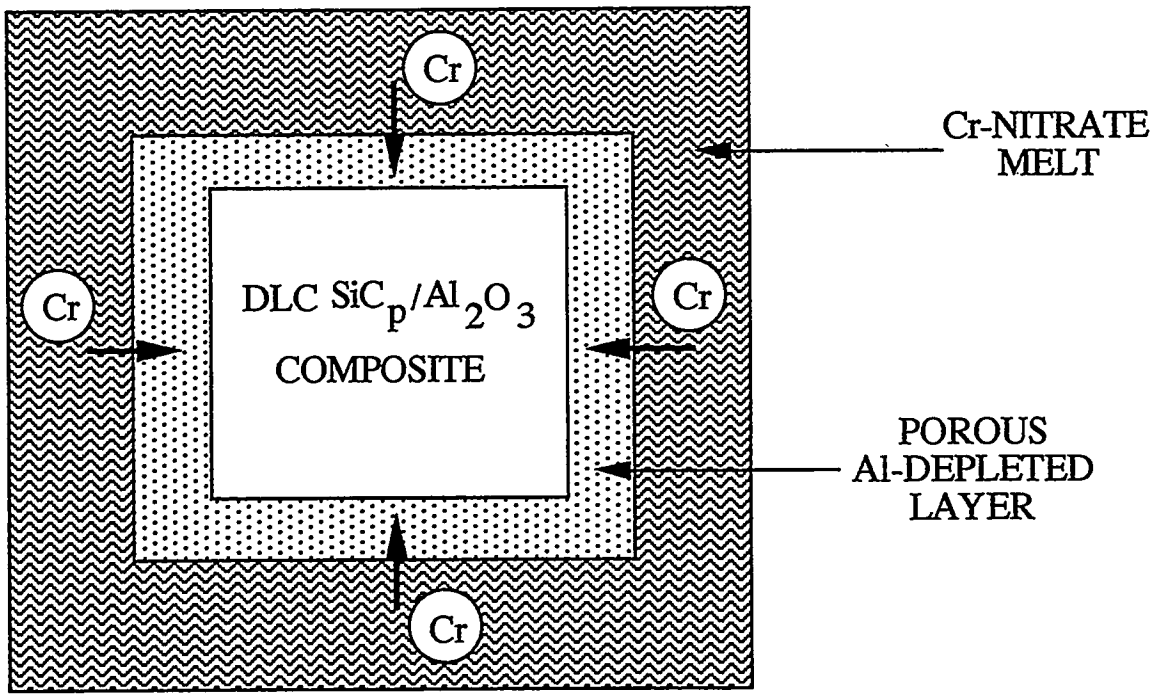

Fig. 8. Schematic of the Cr-infiltration of a DLC SiC_p/Al_2O_3 composite in molten $Cr(NO_3)_3 \cdot 9\,H_2O$.

Table 5. Results of the chemical analysis performed on the Illinois #6 slag from the Baldwin Plant.[8]

Oxides	(a)	(b)	(c)
SiO_2	52.95	53.30	53.30
Al_2O_3	18.47	18.59	18.59
Fe_2O_3	17.48	17.59	17.59
TiO_2	0.71	0.71	0.71
P_2O_5	0.00	0.00	0.00
CaO	7.11	7.16	7.16
MgO	0.98	0.99	0.99
Na_2O	0.00	0.00	0.00
K_2O	1.65	1.66	1.66
SO_3	0.00	0.00	----
Total	99.35	100.00	100.00

(a) Concentrations (wt%) on an ash basis.
(b) Concentrations normalized to a total of 100%.
(c) Concentrations normalized to a SO_3-free basis.

Prior to reaction with the specimens, the slag was heated for 30 min at 800°C, stirred, and reheated for 30 min at 800°C, to burn off any residual carbon and prevent the slag from bubbling and splashing during corrosion tests at 1260°C.[8] In addition, the Cr-infiltrated specimens were ultrasonically cleaned in acetone for 15 min, lightly ground with the 120-grit SiC polishing paper, and recleaned ultrasonically in acetone for 15 min. This surface treatment was undertaken to remove the excess Cr_2O_3 from the specimen surfaces and to restore the circular arc geometry of the specimens. The dimensions and mass of these specimens were measured as well.

The specimens were then positioned on alumina or spinel setter plates and covered with an approximately 3- to 5-mm-thick layer of slag to ensure proper oxygen transport conditions during corrosion tests.[1] The specimen assembly was subsequently placed onto the bottom of an approximately 5-cm-deep partially-stabilized zirconia box and loaded into a SiC globar furnace preheated to a desired temperature. The box was used to prevent the

spilling of molten slag onto the furnace refractory bricks and the heating elements. After a prescribed test time, the specimens were removed from the hot furnace and allowed to cool in air to room temperature. The specimens exposed to the molten slag (1260°C) were sectioned and polished as described above, and analyzed with SEM and EDX to determine the effects of slag on their surfaces.

Corrosion Test in the UND EERC Combustor

Two additional specimens were prepared for a corrosion test conducted in the 220-kW combustor at the UND EERC. The specimens were 25.4-mm-high cylindrical slices taken from the manufacturer-supplied DLC SiC_p/Al_2O_3 heat-exchanger tubes. One of the specimens was provided as-cut, whereas the other was heat treated in a Cr_2O_3 powder bed for 12 h at 1100°C and further equilibrated for 6 h at 1500°C. During the test, the specimens were wedged in the refractory wall of the UND EERC combustor and exposed to the combustor atmosphere at approximately 1260°C for 100 h. The test was successfully completed and the arrival of the corroded specimens from the UND EERC is expected in the near future.[8]

Results and Discussion

Microstructure and Composition of Cr-Infiltrated Specimens

The results of the SEM and EDX analyses performed on the specimens heated in Cr_2O_3 powder bed are summarized in Table 6, indicating the dramatic effects of heat treatment time and temperature on the thickness and continuity of the Cr-rich layer, and the roughness of the resulting specimen surfaces. It appears that a satisfactory compromise among the surface characteristics to warrant further corrosion studies was achieved in specimens No. 1 (2 h at 1000°C in a Cr_2O_3 powder bed, followed by 2 h in air at 1500°C) and No. 4 (12 h at 1100°C in a Cr_2O_3 powder bed, followed by 6 h in air at 1500°C).

The SEM micrographs of the near-surface layers of specimens No. 1 and No. 4 are shown in Figs. 9 (a) and (b), respectively. The EDX spectra corresponding to the brighter and darker phases in specimen No. 4 are shown in Figs. 10 (a), and (b), respectively. Minor quantities of Ca detected within the darker phase indicated that the Ca was used as an additive in the fabrication of the DLC SiC_p/Al_2O_3 composite.[9] The Cr-rich layer observed in the upper portion of the photographs in Fig. 9 consisted of the Cr_2O_3 grains (brighter phase) embedded in a chrome-aluminosilicate matrix (darker phase). The appearance and

Table 6. Summary of the SEM and EDX observations on the specimens infiltrated in a Cr_2O_3 powder bed.

Specimen No.	Average Cr-Layer Thickness (μm)	Cr-Layer Continuity
1	20 ± 2	Yes
2	Outer Wall: 100 ± 10 Inner Wall: 200 ± 60	No
3	200 ± 25	No
4	250 ± 40	Yes

distribution of the darker phase suggested that it had been formed from a liquid and was probably glassy. It is believed that the substantial amount of debris and porosity observed in the upper portion of the Cr-rich layer in specimen No. 4 were in part generated during sample preparation for SEM analysis, involving high-speed cutting and diamond-wheel grinding of the cross sections. However, the porosity observed near the interface between the Cr_2O_3-rich layer and the bulk of the specimen appeared to be intrinsic to the particular method chosen for Cr-infiltration, because the same effect was detected in the specimens reacted with the molten slag (see below).

Even though similar morphologies and compositions were observed on the remaining specimens infiltrated by method (1), extensive regions of discontinuity in the Cr distribution were found in the near-surface layers of specimens Nos. 2 and 3. In addition, the average thickness of the Cr-rich layer in specimen No. 2 was found to be substantially higher (approximately by a factor of 2) on the inner wall of the specimen as compared to the outer wall. This unexpected effect was not observed on any of the remaining specimens infiltrated in a Cr_2O_3 powder bed.

Among the specimens infiltrated with Cr-nitrate (method 2), minor amounts of chromium were detected only on the outer wall of specimen No. 8 (leached for 12 h in concentrated HCl and equilibrated for 6 h at 1500°C). The SEM photograph of this

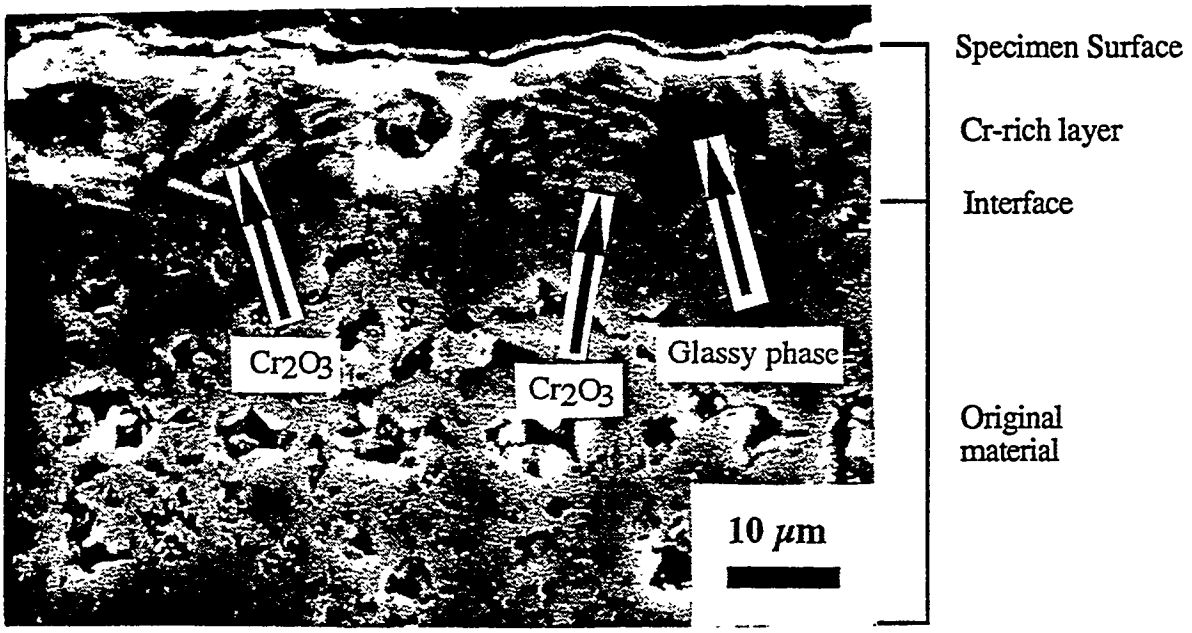

(a)

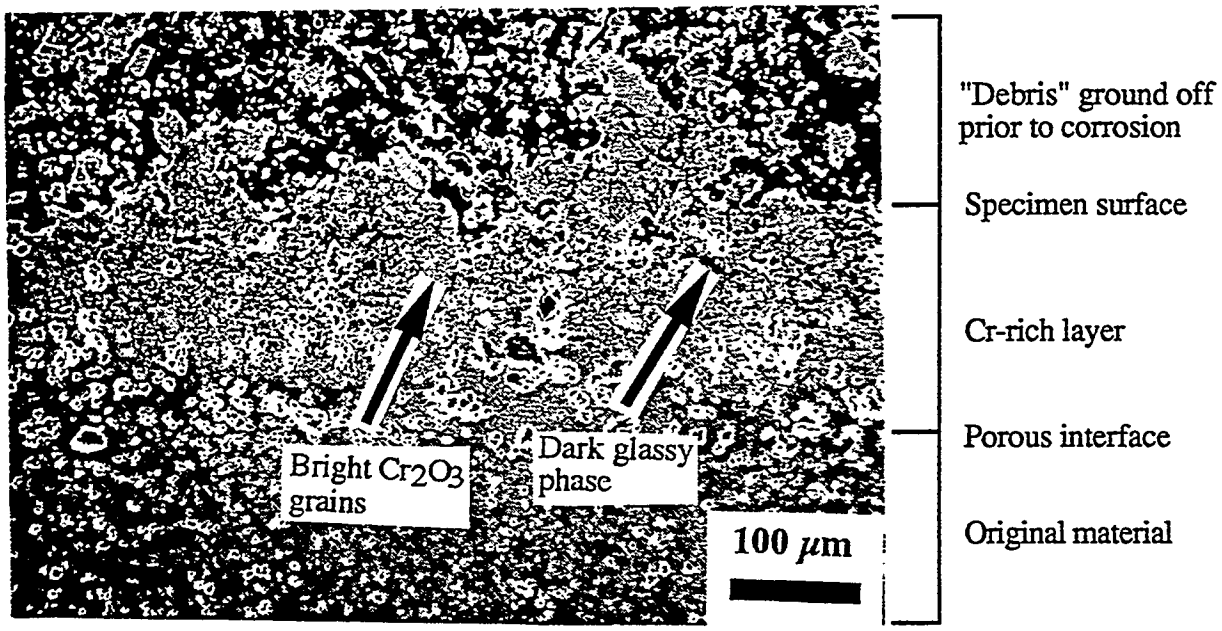

(b)

Fig. 9. SEM photographs of the near surface layers of a DLC SiC_p/Al_2O_3 composite infiltrated in a Cr_2O_3 powder bed for (a) 2 h at 1000°C and equilibrated for 2 h at 1500°C, and (b) 12 h at 1100°C and equilibrated for 6 h at 1500°C.

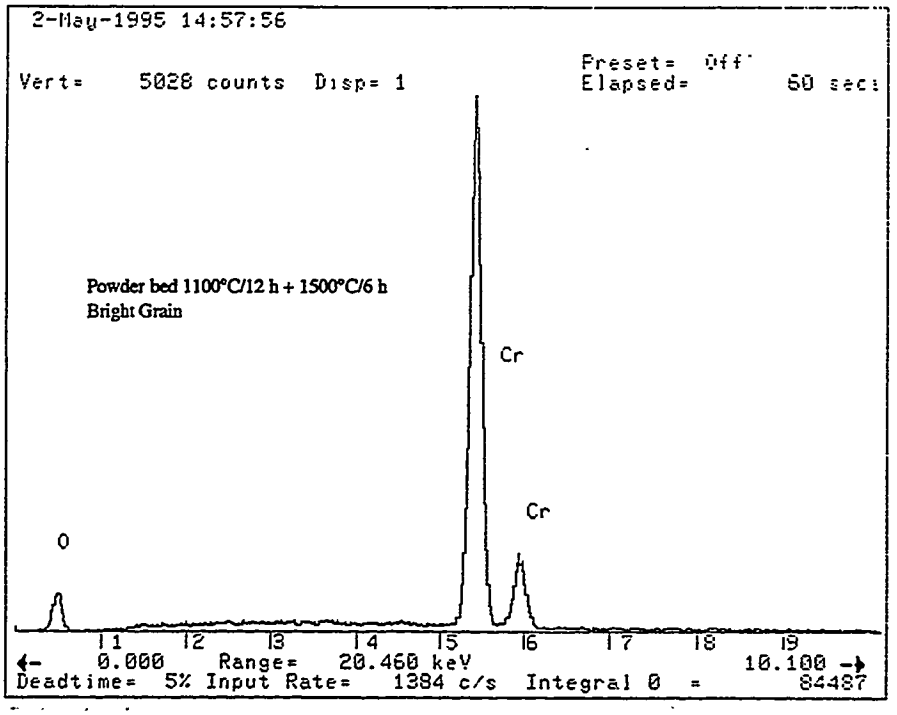

(a)

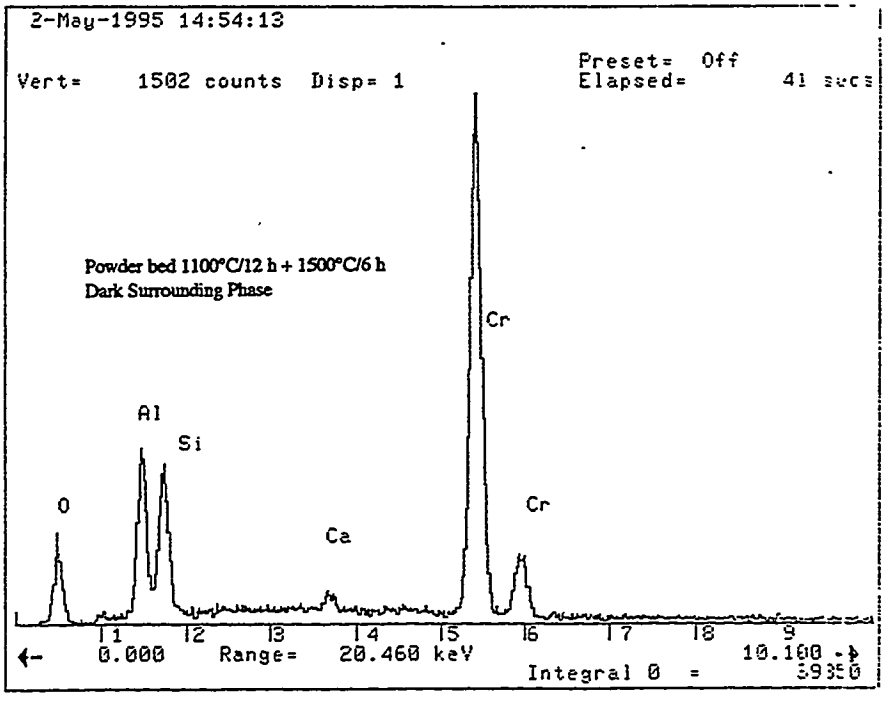

(b)

Fig. 10. EDX spectra corresponding to (a) the bright phase, and (b) the dark phase observed in the upper portion of Fig. 9 (b).

specimen is presented in Fig. 11, indicating the formation of a 50 ± 8 μm thick modified surface layer. This layer was only slightly enriched with Cr, as shown in the EDX spectrum obtained from a randomly selected point within this layer (Fig. 12). Apparently, the surface porosity created in specimens Nos. 5 through 8 was insufficient to allow any substantial penetration of molten Cr-nitrate by capillary action at 80°C. It is possible that an additional heat-treatment step at 1100°C, after the decomposition of the nitrate had been completed, might have improved the infiltration and yielded higher surface concentration of chromium in specimen No. 8. At this stage, however, it was concluded that the Cr-nitrate treatment did not yield required surface characteristics to expect an improvement in corrosion resistance.

Microstructure and Composition of Specimens Reacted with Molten Slag

The specimens infiltrated in a Cr_2O_3 powder bed (either for 2 h at 1000°C, or 12 h at 1100°C), along with several Cr-free specimens to be used for comparison, were selected for corrosion tests. By weighing the Cr-infiltrated specimens before and after infiltration and the 1500°C surface equilibration, it was determined that the specimens infiltrated at 1000°C contained 0.7 to 1 wt% Cr_2O_3, whereas those infiltrated at 1100°C contained 3 to 4 wt% Cr_2O_3. The corresponding concentrations within the Cr-rich layers were calculated to be approximately 65 and 25 wt% Cr_2O_3, respectively. The calculation was based on the thicknesses reported in Table 6, and the density of Cr_2O_3 of 5.21 g/cm^3.

The microstructures of the Cr-free specimens reacted with the molten slag at 1260°C are shown in cross section in Fig. 13. Even though considerable porosity was present within the layer of slag due to bubble formation, the interfaces between the slag and the specimens were otherwise found to be remarkably smooth and unaffected by corrosion after either a 2-h (Fig. 13 (a)) or 20-h (Fig. 13 (b)) exposure. In both cases, a bright pearl-like phase crystallized within the slag layer, exhibiting a tendency to segregate towards the surface of the slag layer.

A significant difference was observed in the compositions of the pearl-like phase after a 2-h and 20-h exposure, as seen in the corresponding EDX spectra of the individual bright grains shown in Figs. 14 (a) and (b), respectively. After a 2-h exposure, the apparent composition of the bright phase corresponded to a (Ca,K) iron-aluminosilicate, with the levels of Fe significantly above those expected from the slag (see Table 5). After the 20-h exposure, the composition was nearly pure Fe_2O_3,[10] with minor amounts of alumina and titania in solid solution. Further examination of the crystallite size,

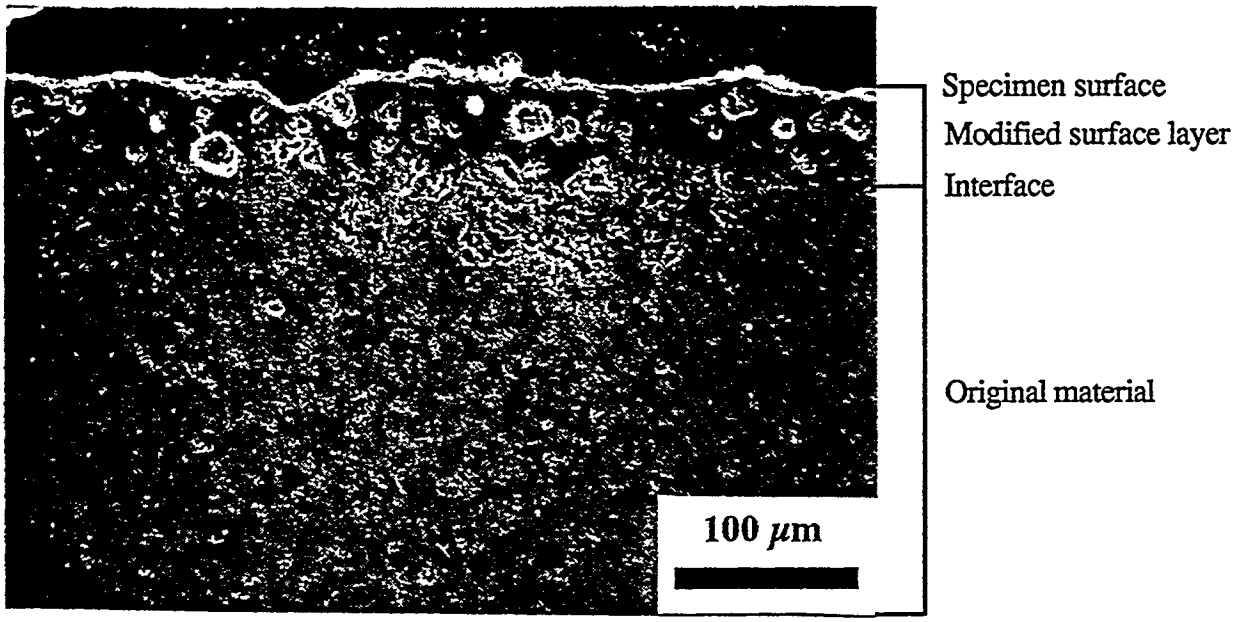

Fig. 11. SEM photograph of a near-surface layer of the outer wall of a DLC SiC_p/Al_2O_3 composite etched for 12 h in concentrated HCl, infiltrated with $Cr(NO_3)_3 \cdot 9 H_2O$ for 24 h at 80°C, and equilibrated for 6 h at 1500°C.

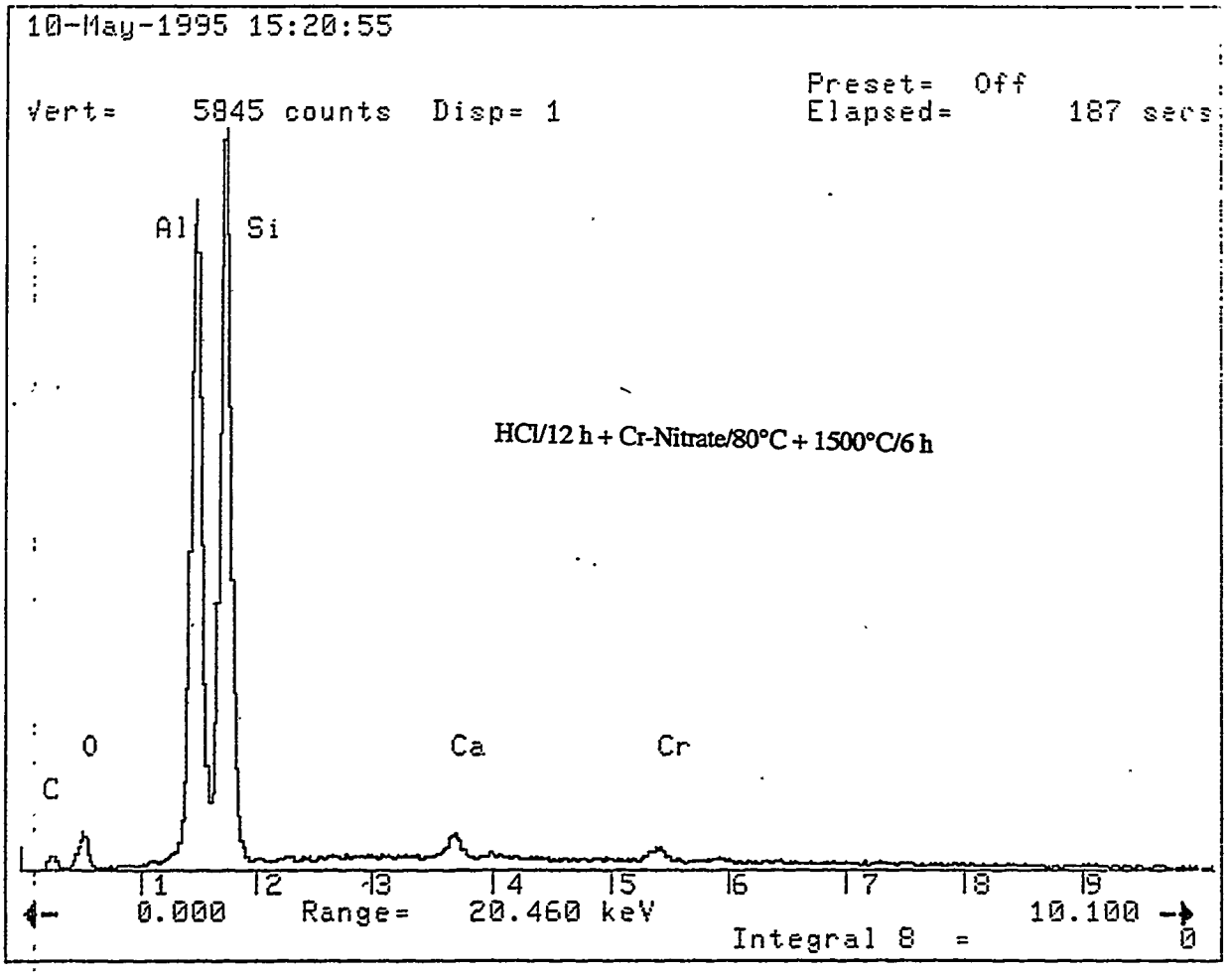

Fig. 12. EDX spectrum obtained from a randomly selected spot within the modified surface layer shown in the upper portion of Fig. 11.

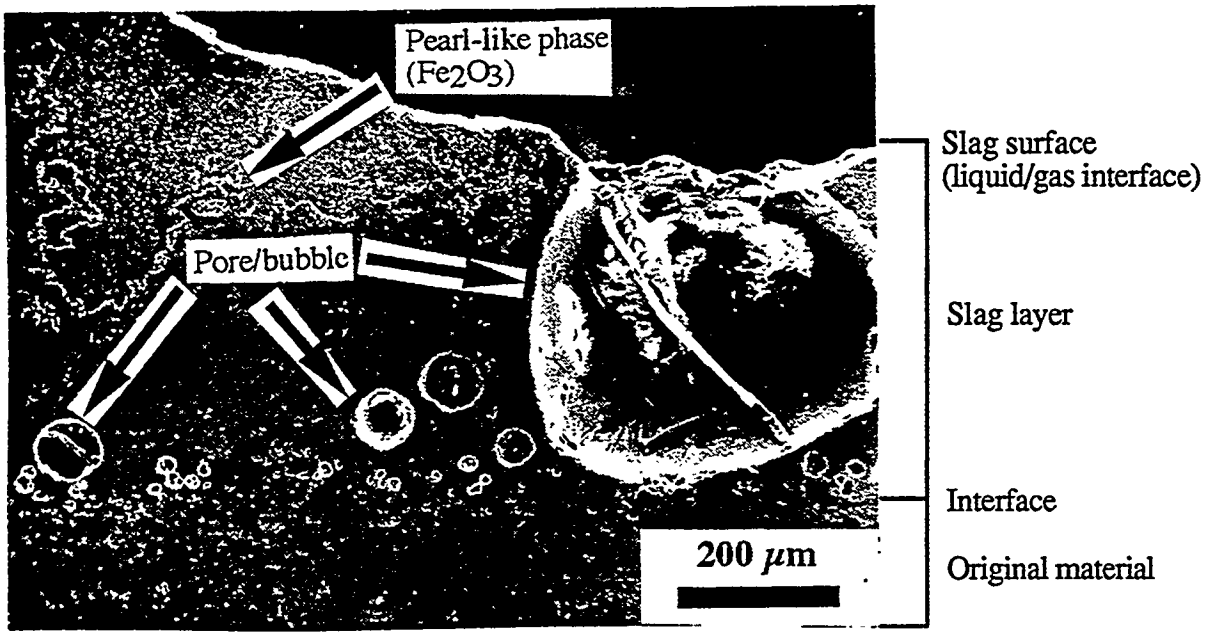

(a)

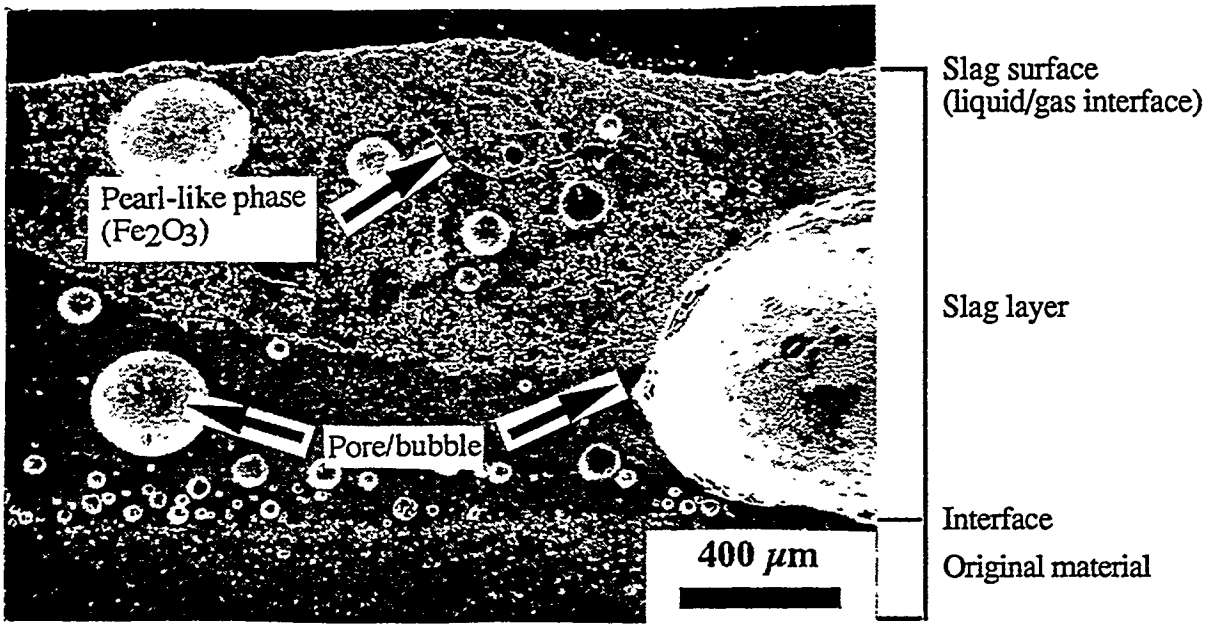

(b)

Fig. 13. SEM photographs of the near surface layers of a Cr-free DLC SiC_p/Al_2O_3 composite reacted with molten Illinois #6 slag at 1260°C for (a) 2 h, and (b) 20 h.

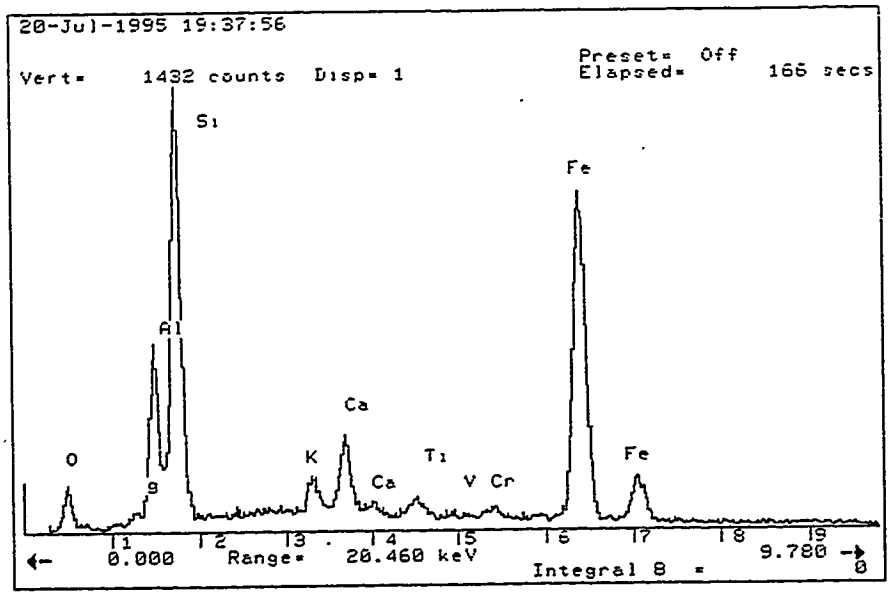

(a)

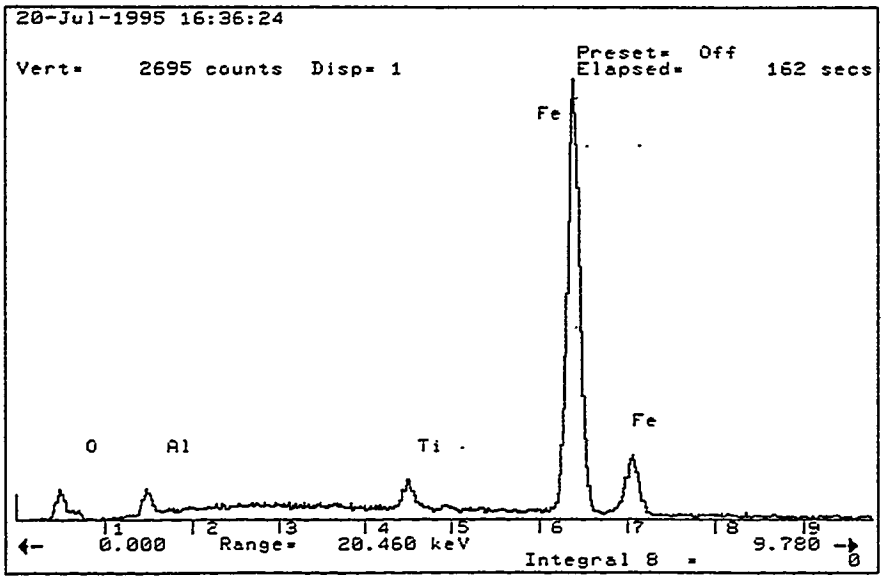

(b)

Fig. 14. EDX spectra corresponding to the bright, pearl-like phase observed (a) in Fig. 13 (a), and (b) in Fig. 13 (b).

morphology and composition of the pearl-like phase suggested that already after the 2-h exposure this phase was probably pure Fe_2O_3. It is believed that in this case the spatial resolution of the EDX analysis was insufficient to avoid the X-ray fluorescence signal from the surrounding slag. In both cases, an independent confirmation of the presence of Fe_2O_3 within the slag will be sought by X-ray diffraction. In addition, to test whether the Fe_2O_3 formation within the slag may in any way be related to the presence of the DLC SiC_p/Al_2O_3 substrate or its potential corrosion, a heat treatment of the slag alone will be conducted at 1260°C and the results compared to those reported here.

The EDX analysis of the darker phase surrounding the pearl-like grains within the slag layer in both cases qualitatively corresponded to the slag composition given in Table 5. However, the amount of Fe was found to increase towards the surface of the slag layer, suggesting the tendency for Fe to segregate near the liquid/gas interface during this corrosion test.

The microstructures of the Cr-infiltrated specimens exposed to the molten slag at 1260°C are shown in cross section in Figs. 15 (a) and (b) for a 2-h and 20-h exposure, respectively. In both cases, the EDX analysis revealed the presence of a Cr-rich bright phase near the porous interface between the Cr-affected zone and the original material, with a morphology similar to that observed on the Cr-infiltrated specimens prior to corrosion tests (Fig. 9 (b)). Despite the porosity, the transition from the specimen bulk into the Cr-rich layer, and further into the Fe-containing dark layer of slag near the top of Figs. 15, appeared to be smooth and continuous. It should be noted, however, that rearrangement and segregation of the Cr-rich grains, both indicative of corrosion, occurred toward the surface of the molten slag layer.

Considerable differences were detected in the compositions of the bright and the dark phase after a 2-h and 20-h exposure to molten slag. The EDX spectra for the bright phase are compared in Fig. 16. After a 2-h exposure (Fig. 16 (a)), nearly pure Cr_2O_3 is observed.[11] After a 20-h exposure (Fig. 16 (b)), a large amount of Fe was found to diffuse into the bright phase, which had a composition corresponding to a chrome-iron-aluminosilicate. A corrosion-indicative Fe enrichment within the bright grains observed in Fig. 15 (b) occurred at the expense of the dark, glassy phase surrounding the Cr-rich grains, as evident from the EDX spectra shown in Fig. 17. After a 2-h exposure (Fig. 17 (a)), the dark phase in the upper portion of Fig. 15 (a) had a complex composition, qualitatively corresponding to the original slag composition listed in Table 5, doped with

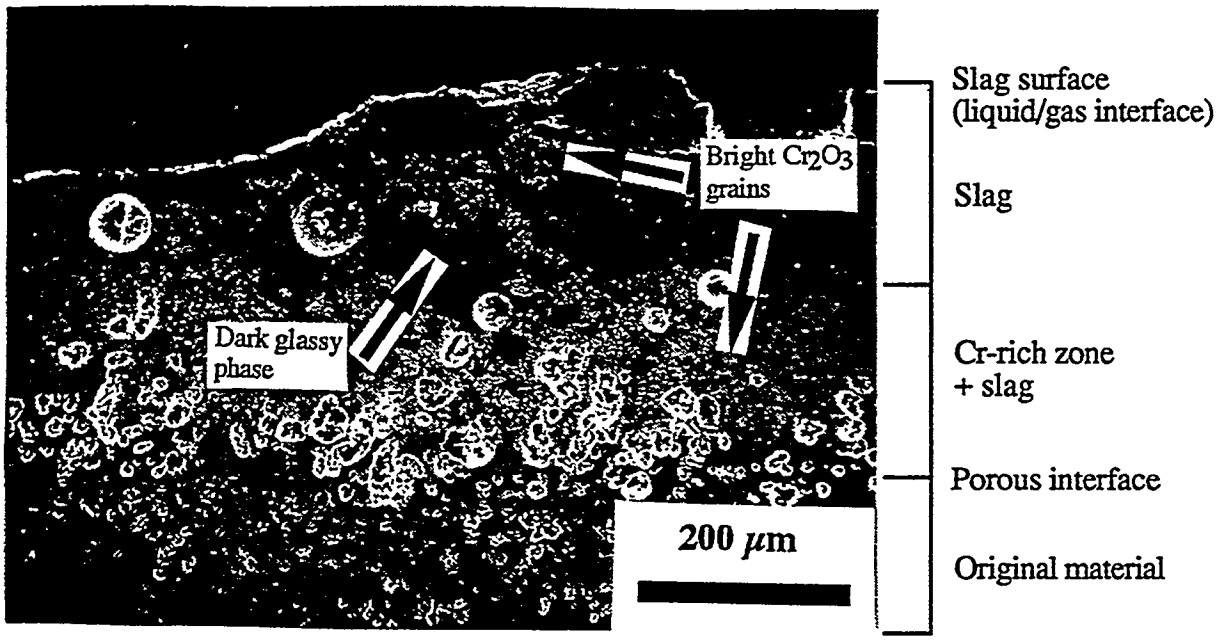

(a)

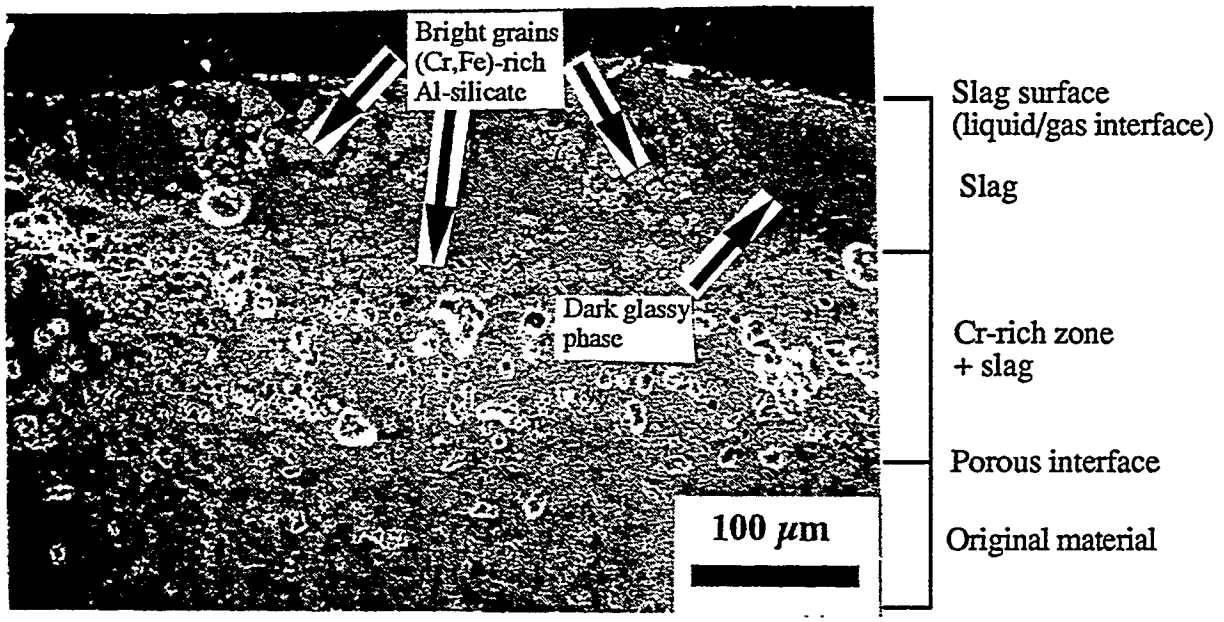

(b)

Fig. 15. SEM photographs of the near surface layers of a DLC SiC_p/Al_2O_3 composite infiltrated in a Cr_2O_3 powder bed for 12 h at 1100°C, equilibrated for 6 h at 1500°C, and reacted with molten Illinois #6 slag at 1260°C for (a) 2 h, and (b) 20 h.

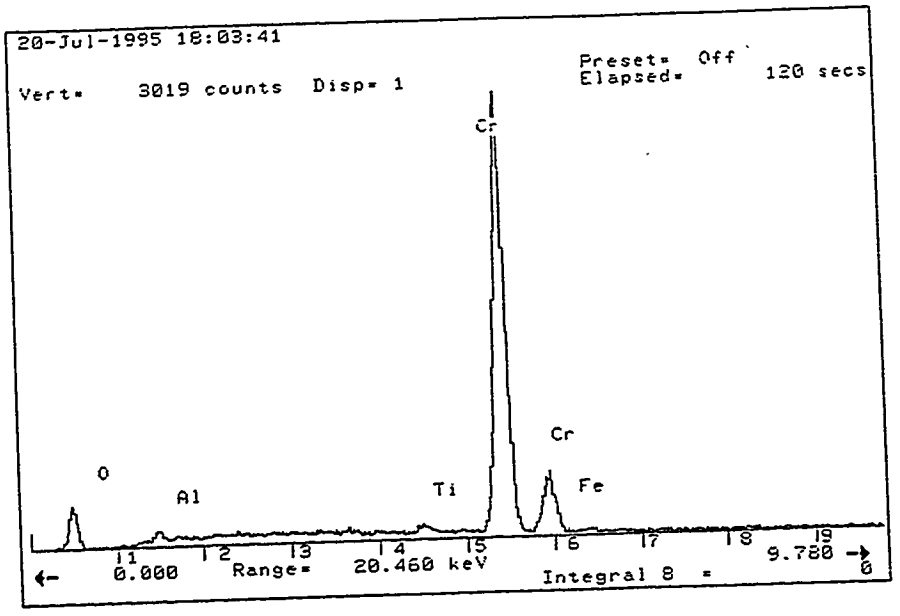

(a)

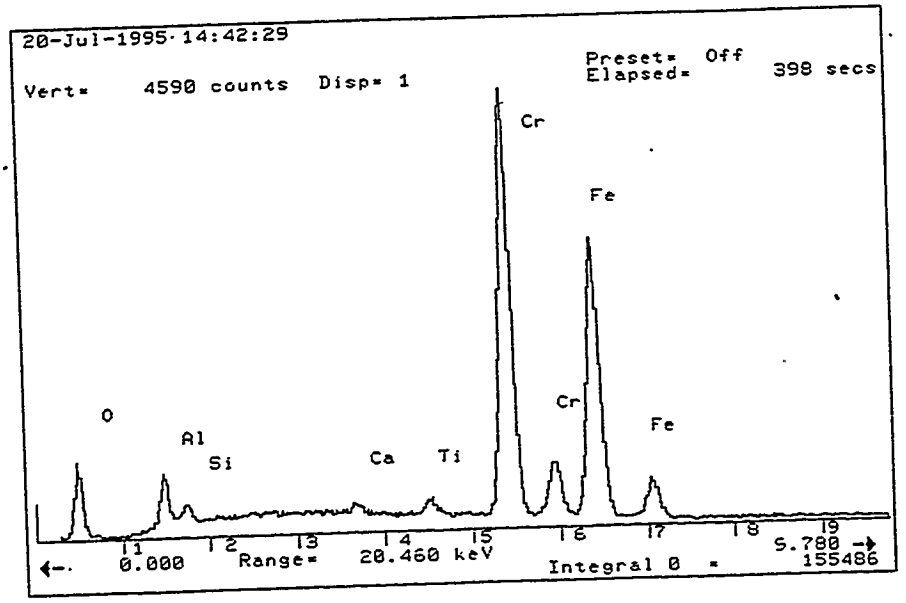

(b)

Fig. 16. EDX spectra obtained from the bright grains shown (a) in Fig. 15 (a), and (b) in Fig. 15 (b).

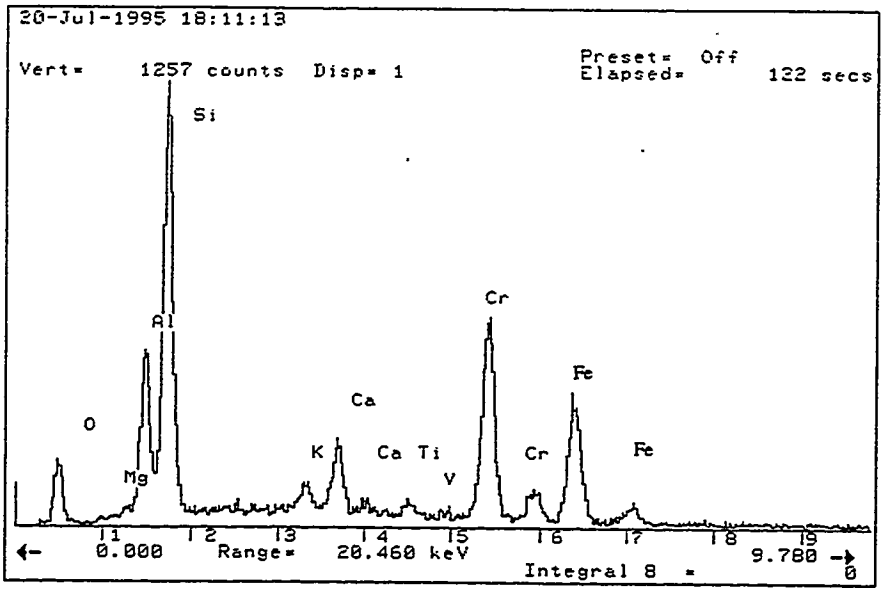

(a)

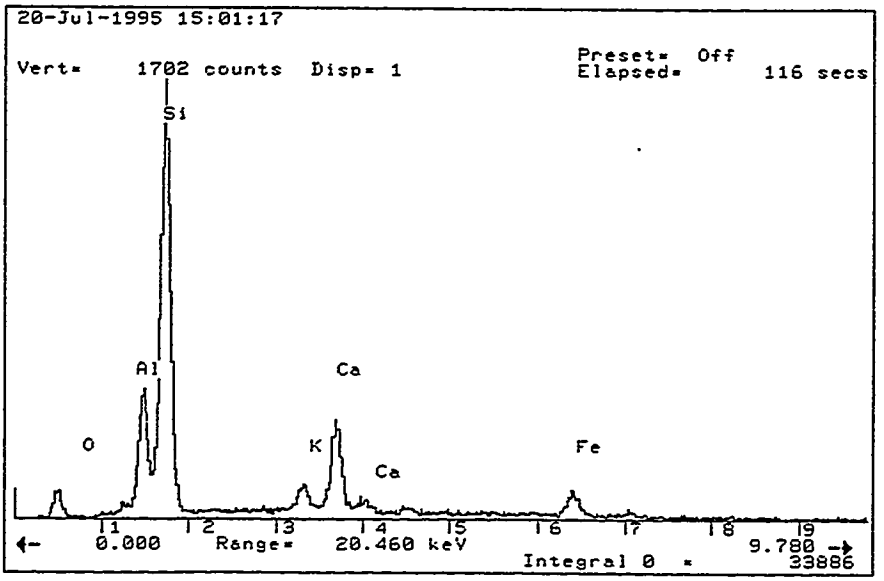

(b)

Fig. 17. EDX spectra obtained from the dark, glassy phase shown within the layer of slag (a) in Fig. 15 (a), and (b) in Fig. 15 (b).

Cr. After a 20-h exposure, however (Fig. 17 (b)), the glassy phase became almost completely depleted in Fe, and entirely free of Cr (within the detection limit of the EDX).

Selection of Another Candidate Coating Material

The most up-to-date information obtained from the contacts in the research and industrial communities indicated that the bulk of the DoE-funded efforts on corrosion protection of heat exchanger tubes was geared toward developing alumina and mullite coatings on SiC.[9, 12, 13] Because of a complete solid solubility of Cr_2O_3 in Al_2O_3, it is suggested that Cr-doping be attempted in these two coating materials to test whether an improvement in corrosion resistance can be obtained.

Summary and Future Work on Heat Exchanger Materials

The Cr-infiltration of a DLC SiC_p/Al_2O_3 composite heat exchanger material in a Cr_2O_3 powder bed resulted in continuous Cr-rich layers with thicknesses ranging from 20 to 250 μm. The Cr-infiltration in molten $Cr(NO_3)_3 \cdot 9\ H_2O$ was found to be inadequate to produce any substantial penetration of Cr into the composite surfaces. The composite specimens infiltrated in a Cr_2O_3 powder bed, along with several Cr-free specimens used for comparison, were exposed to the molten Illinois #6 slag for 2 and 20 h at 1260°C. In the Cr-free specimens, the segregation of Fe and the precipitation of Fe_2O_3 were detected near the liquid/gas interface, but no evidence of corrosion was present. In the Cr-infiltrated specimens, however, corrosion was evident, since a rearrangement and segregation of the Cr-rich grains occurred toward the surface of the molten slag. In addition, evidence of the diffusion of major quantities of Fe was observed from the liquid slag into the Cr-rich layer formed by infiltration. Finally, it is suggested that Cr_2O_3-doping of alumina and mullite protective coatings on SiC heat exchanger tubes be attempted in order to improve the effectiveness of these coatings against molten coal-ash slags.

By the end of FY 1994/95 (August 31, 1995) the SEM and EDX analyses of the remaining specimens exposed to the Illinois #6 slag will be completed. In addition, the mass change of the corroded specimens as a function of time at 1093° and 1260°C will be measured. Long-term plans for further activities have been proposed in the Work Statement for FY 1995/96, focusing on the following areas: (1) distinguishing and separating the simultaneous effects of Cr-diffusion, surface oxidation, and surface recession during the reaction of composite surfaces with molten slag; (2) measuring the

room-temperature strength of the corroded Cr-infiltrated heat-exchanger tubes; and (3) preparing bulk test specimens of Cr-doped mullite and exposing them to a coal-ash slag for various times and temperatures.

ACKNOWLEDGMENTS

We would like to thank D. Pysher (3M Co.), P. Gray (DuPont Lanxide Composites Inc.), and D. Landini (DuPont Lanxide Composites Inc.) for providing the samples for this work, and J.P. Hurley (UND EERC) for helping us obtain the ash and slags for corrosion testing. Helpful discussions with D. Stinton (ORNL) are also gratefully acknowledged.

REFERENCES

1. J. P. Hurley, "Factors Affecting the Corrosion Rates of Ceramics in Coal Combustion Systems," to be published in the Proceedings of the Ninth Annual Fossil Energy Materials Conference.

2. B. Cheynet, "MICROTHERM - Thermochemical Databank System for Inorganic Substances," © 1989 by Thermodata.

3. G. Eriksson, K. Hack and M. Philipps, ChemSage, Version 3.0, © 1993 by G. Eriksson (GTT mbh, Kaiserstasse 100, 5120 Herzogenrath 3, Germany).

4. K. Breder and V.J. Tennery, "Materials Support for the Development of High Temperature Advanced Furnaces (HITAF)—A Comparison of Selected Mechanical Properties for Three SiC-Based Ceramics"; A Discussion of DoE-Sponsored Fossil Energy Research Projects. The Pennsylvania State University, University Park, PA (1994).

5. C. R. Kennedy, "Reinforced Ceramics Via Oxidation of Molten Metals," *Ceram. Ind.*, 26–29, December 1994.

6. K. H. Sandhage and G. J. Yurek, Indirect Dissolution of $(Al,Cr)_2O_3$ in CaO–MgO–Al_2O_3–SiO_2 (CMAS) Melts," *J. Am. Ceram. Soc.*, **74** [8] 1941–54 (1991).

7. W. A. Kern, M. J. McNallan and R. E. Tressler, "Oxidation and Corrosion of SiC/Al/Al_2O_3 Composites Fabricated by Directed Metal Oxidation in Sodium Silicate at Elevated Temperatures," *J. Am. Ceram. Soc.* (to be published).

8. J. P. Hurley, personal communication.

9. D. J. Landini, personal communication.

10. A. Muan, "Phase Equilibria at High Temperatures in Oxide Systems Involving Changes in Oxidation States," *Am. J. Sci.*, **256**, 171–207, 1958.

11. Phase Diagrams for Ceramists, Figures 4152 and 5002.

12. V. K. Sarin and R. Mulpury, "Mullite Coatings for Corrosion Protection of Silicon Carbide" (abstract); presented at the Ninth Annual Conference on Fossil Energy Materials. Oak Ridge, TN, May 16 to 18, 1995.

13. D. P. Stinton, personal communication.

DISTRIBUTION

AIR PRODUCTS AND CHEMICALS
P.O. Box 538
Allentown, PA 18105
S. W. Dean

ALBERTA RESEARCH COUNCIL
Oil Sands Research Department
P.O. Box 8330
Postal Station F
Edmonton, Alberta
Canada T6H5X2
L. G. S. Gray

ALLISON GAS TURBINE DIVISION
P.O. Box 420
Indianapolis, IN 46206-0420
P. Khandelwal (Speed Code W-5)
R. A. Wenglarz (Speed Code W-16)

ARGONNE NATIONAL LABORATORY
9700 S. Cass Avenue
Argonne, IL 60439
K. Natesan

ARGONNE NATIONAL LABORATORY-WEST
P.O. Box 2528
Idaho Falls, ID 83403-2528
S. P. Henslee

AVCO RESEARCH LABORATORY
2385 Revere Beach Parkway
Everett, MA 02149
R. J. Pollina

BABCOCK & WILCOX
1562 Beeson St.
Alliance, OH 44601
T. I. Johnson

BABCOCK & WILCOX
Domestic Fossil Operations
20 South Van Buren Avenue
Barberton, OH 44023
M. Gold

BRITISH COAL CORPORATION
Coal Technology Development Division
Stoke Orchard, Cheltenham
Glocestershire, England GL52 4ZG
J. Oakey

CANADA CENTER FOR MINERAL & ENERGY TECHNOLOGY
568 Booth Street
Ottawa, Ontario
Canada K1A OG1
R. Winston Revie
Mahi Sahoo

ELECTRIC POWER RESEARCH INSTITUTE
P.O. Box 10412
3412 Hillview Avenue
Palo Alto, CA 94303
W. T. Bakker
J. Stringer
R. Wolk

EUROPEAN COMMUNITIES JOINT RESEARCH CENTRE
Petten Establishment
P.O. Box 2
1755 ZG Petten
The Netherlands
M. Van de Voorde

FOSTER WHEELER DEVELOPMENT CORPORATION
Materials Technology Department
John Blizard Research Center
12 Peach Tree Hill Road
Livingston, NJ 07039
J. L. Blough

GAS RESEARCH INSTITUTE
8600 West Bryn Mawr Avenue
Chicago, IL 60631
H. S. Meyer

IDAHO NATIONAL ENGINEERING LABORATORY
P. O. Box 1625
Idaho Falls, ID 83415
A. B. Denison

LAWRENCE LIVERMORE NATIONAL LABORATORY
P.O. Box 808, L-325
Livermore, CA 94550
W. A. Steele

MOBIL RESEARCH & DEVELOPMENT CORPORATION
P. O. Box 1026
Princeton, NJ 08540
R. C. Searles

NATIONAL MATERIALS ADVISORY BOARD
National Research Council
2101 Constitution Avenue
Washington, DC 20418
K. M. Zwilsky

OAK RIDGE NATIONAL LABORATORY
P.O. Box 2008
Oak Ridge, TN
P. T. Carlson
N. C. Cole
R. R. Judkins
R. A. Lawson (8 copies)
D. P. Stinton
P. F. Tortorelli
I. G. Wright

RISOE NATIONAL LABORATORY
P.O. Box 49
DK-4000
Roskilde, Denmark
Aksel Olsen

SHELL DEVELOPMENT COMPANY
P. O. Box 1380
Houston, TX 77251-1380
L. W. R. Dicks

SOUTHWEST RESEARCH INSTITUTE
6620 Culebra Road
P.O. Drawer 28510
San Antonio, TX 78284
F. F. Lyle, Jr.

TENNESSEE VALLEY AUTHORITY
Energy Demonstration & Technology
MR 2N58A
Chattanooga, TN 37402-2801
C. M. Huang

TENNESSEE VALLEY AUTHORITY
1101 Market Street
3A Missionary Ridge
Chattanooga, TN 37402-2801
A. M. Manaker

THE MATERIALS PROPERTIES COUNCIL, INC.
United Engineering Center
345 E. Forty-Seventh Street
New York, NY 10017
M. Prager

UNIVERSITY OF TENNESSEE AT KNOXVILLE
Materials Science and Engineering Department
Knoxville, TN 37996
R. A. Buchanan

WESTERN RESEARCH INSTITUTE
365 N. 9th Street
P.O. Box 3395
University Station
Laramie, WY 82071
V. K. Sethi

WESTINGHOUSE ELECTRIC CORPORATION
Research and Development Center
1310 Beulah Road
Pittsburgh, PA 15235
S. C. Singhal

DOE
DOE OAK RIDGE OPERATIONS
P. O. Box 2001
Oak Ridge, TN 37831
Assistant Manager for Energy Research and Development

DOE
DOE OAK RIDGE OPERATIONS
P. O. Box 2008
Building 4500N, MS 6269
Oak Ridge, TN 37831
E. E. Hoffman

DOE
OFFICE OF BASIC ENERGY SCIENCES
Materials Sciences Division
ER-131, GTN
Washington, DC 20545
J. B. Darby

DOE
OFFICE OF FOSSIL ENERGY
FE-72
19901 Germantown Road
Germantown, MD 20874-1290
J. P. Carr

DOE
MORGANTOWN ENERGY TECHNOLOGY
CENTER
P.O. Box 880
Morgantown, WV 26505
R. C. Bedick
D. C. Cicero
F. W. Crouse, Jr.
N. T. Holcombe
W. J. Huber
J. E. Notestein

DOE
PITTSBURGH ENERGY TECHNOLOGY
CENTER
P.O. Box 10940
Pittsburgh, PA 15236
A. L. Baldwin
G. V. McGurl
T. M. Torkos

DOE
OFFICE OF SCIENTIFIC AND TECHNICAL
INFORMATION
P. O. Box 62
Oak Ridge, TN 37831
For distribution by microfiche as shown in
DOE/TIC-4500, Distribution Category:
UC-114 (Coal Based Materials and Components)

ADDITIONAL DISTRIBUTION

a. External

1. John P. Hurley
Energy and Environmental Research Center
University of North Dakota
P.O. Box 9018
Grand Forks, ND 58202-9018

2. Paul E. Gray
DuPont Lanxide Composites
400 Bellevue Road
Newark, DE 19714

3. William A. Kern
PPG Industries, Inc.
Aircraft Products Division
Huntsville, AL 35811

4. Dennis J. Landini
Lanxide Corporation
1300 Marrows Road
Box 6077
Newark, DE 19714-6077

5. Doug Pysher
3M Co.
3M Center
Bldg. 201-4N-01
St. Paul, MN 55144-1000

6. Kenneth H. Sandhage
477 Watts Hall
Department of Materials Science and Engineering
Ohio State University
116 W. 19th Ave.
Columbus, OH 43210

b. Internal:

1. E.R. Kupp
2. R.L. Shelleman
3. K.E. Spear
4. R.E. Tressler
5. M.F. Trubelja